SCIENTIFIC REPORTS

OPEN

SUBJECT AREAS:
SUB-WAVELENGTH OPTICS
NANOPHOTONICS AND PLASMONICS
NANOPARTICLES

Received
19 June 2013

Accepted
8 October 2013

Published
25 October 2013

Correspondence and requests for materials should be addressed to T.I. (t-iida@21c.osakafu-u.ac.jp) or S.I. (sito@chem.es.osaka-u.ac.jp)

Selective Optical Assembly of Highly Uniform Nanoparticles by Doughnut-Shaped Beams

Syoji Ito[1,2,3], Hiroaki Yamauchi[1,2], Mamoru Tamura[4,5], Shimpei Hidaka[4,5], Hironori Hattori[4,5], Taichi Hamada[4,5], Keisuke Nishida[4,5], Shiho Tokonami[4], Tamitake Itoh[6], Hiroshi Miyasaka[1,2] & Takuya Iida[3,4]

[1]Division of Frontier Materials Science, Graduate School of Engineering Science, Osaka University, Toyonaka, Osaka 560-8531, Japan, [2]Center for Quantum Materials Science under Extreme Conditions, Osaka University, Toyonaka, Osaka 560-8531, Japan, [3]PRESTO, Japan Science and Technology Agency, 4-1-8 Honcho, Kawaguchi, Saitama 332-0012, Japan, [4]Nanoscience and Nanotechnology Research Center, Resaearch Organization for the 21st Century, Osaka Prefecture University, 1-2, Gakuencho, Nakaku, Sakai, Osaka 599-8570, Japan, [5]Graduate School of Engineering, Osaka Prefecture University, 1-1, Gakuen-cho, Nakaku, Sakai, Osaka 599-8531, Japan, [6]Health Research Institute, National Institute of Advanced Industrial Science and Technology (AIST), Takamatsu, Kagawa 761-0395, Japan.

A highly efficient natural light-harvesting antenna has a ring-like structure consisting of dye molecules whose absorption band changes through selective evolutionary processes driven by external stimuli, i.e., sunlight depending on its territory and thermal fluctuations. Inspired by this fact, here, we experimentally and theoretically demonstrate the selective assembling of ring-like arrangements of many silver nanorods with particular shapes and orientations onto a substrate by the light-induced force of doughnut beams with different colours (wavelengths) and polarizations in conjunction with thermal fluctuations at room temperature. Furthermore, the majority of nanorods are electromagnetically coupled to form a prominent red-shifted collective mode of localized surface plasmons resonant with the wavelength of the irradiated light, where a spectral broadening also appears for the efficient broadband optical response. The discovered principle is a promising route for "*bio-inspired selective optical assembly*" of various nanomaterials that can be used in the wide field of nanotechnology.

Assembly processes driven by fluctuations and dissipation[1] under external perturbations have created a variety of biological and non-biological nanosystems[2–4]. For instance, a natural light-harvesting antenna (LHA) in a bacterium has a ring-like structure consisting of dye molecules[5,6] whose absorption band has been changing through selective evolutionary processes[7] driven by external stimuli, i.e., sunlight and thermal fluctuations depending on its territory. Paying attention to this fact, we pose a question: "*Can we selectively assemble non-biological nanomaterials exhibiting specific spectroscopic properties by tailored light and fluctuations?*"

In this paper, to shed light on this question, we experimentally and theoretically demonstrate the selective assembling of ring-like arrangements of many anisotropic nanoparticles (NPs) with particular shapes and orientations from a group of NPs with various shapes by light-induced forces in conjunction with thermal fluctuations at room temperature. To clarify the possibility of the above-mentioned selective production of an optically-assembled structure of NPs with high-rotational symmetry and efficient optical properties analogous to LHA in natural photosynthetic systems, we investigated the dynamics of silver (Ag) nanomaterials experiencing light-induced force of designed light fields under the random collisions of environmental molecules. In previous works, such a light-induced force has allowed us to manipulate micronparticles[8], semiconductor and metallic NPs[9–13], and to control the local photopolymerization[14]. Also, there are reports with specialized light fields, for example, the transport of NPs with modulated standing wave[15], the manipulation of multiple particles by holographic tweezers[16] or femtosecond pulses[17], and the trapping of molecules by localized field between metallic NPs[18]. However, for the above-mentioned selective assembling as the purpose of this study, we particularly pay attention to light-induced force under the irradiation of a laser beam with high rotational symmetry and unique polarization distributions, i.e., axially-symmetric polarized vector beams (APVBs)[19,20]. Although several experiments about optical trapping of a small number of gold nanorods (NRs)[21–23] and semiconductor core-shell NRs[24]

were reported, there is no work demonstrating selective extraction and assembling of many Ag NRs with a uniform shape. In addition, since selective production of Ag NRs with a particular aspect ratio is difficult and the synthesis method is limited[25], our method would be useful for this purpose. Furthermore, as it can be expected that assembled metallic nanomaterials exhibit the collective interaction of localized surface plasmons (LSPs) leading to strong radiative coupling[13,26–28], we have measured dark-field scattering spectra of the optically-assembled structures and theoretically evaluated the spectra in terms of the mutual coupling of Ag NRs.

Results

The experimental configuration of the present study for the selective assembling of plasmonic nanomaterials is shown in Figure 1. TEM_{00} continuous wave (CW) lasers with different wavelengths (660 nm and 1064 nm) were used as light sources for optical manipulation. Since Ag nanostructures show a strong optical response with sharp LSP resonance (owing to a small nonradiative damping[29]) and are suitable for optical manipulation at room temperature, Ag NPs were prepared as target materials by a reduction method[30]. The transverse mode and polarization of each laser was converted into a doughnut-like beam with either azimuthal or radial polarization. Irradiation with the doughnut-like beams for several minutes resulted in the deposition of many Ag NPs on the surface of a glass slide (see **Methods** for more details). Fig. 1c shows a dark-field scattering image of 3 × 3 doughnut-like microstructures produced by several minutes irradiation of a radially polarized doughnut beam at 1064 nm per each microstructure (assembling process of a single doughnut-like microstructure is recorded in monochromatic movie in **Supplementary Movie S1**). Surprisingly, the majority of produced microstructures exhibit orange colour although the LSP resonance of individual Ag NPs is in the wavelength region of purple (Fig. 1b). The following passages describe the detail of our research to clarify what phenomena occurred under the irradiation of the doughnut beam.

It was confirmed by transmission electron microscopy (TEM), that most of the prepared Ag NPs had shapes with low aspect ratios; a small number of nanostructures with high aspect ratios (>3) were also observed (Fig. 2a). This is consistent with the extinction spectrum shown in Fig. 1b. The detailed geometric properties of the NPs were observed under high magnification (inset of Fig. 2a); the magnified TEM image shows various shapes existed, for example, spherical, triangular, and rod-like. However, after irradiation by the doughnut-like beam (azimuthal or radial polarization) for 6 minutes under the conditions illustrated in Fig. 1a, nanostructures with specific characteristics were manipulated according to the properties of the beam. As a result, depending on laser wavelengths, many Ag NRs with different aspect ratios were strongly fixed on the glass substrate even after washing with ultrapure water (Figs. 2b–2e). For the both wavelengths, the majority of Ag NRs were concentrated in the region corresponding to the spatial distribution of the doughnut-like intensity distribution of diameter ~2 μm. The remarkable point is that NRs of low aspect ratio (~2) were selectively fixed by the laser of 660 nm wavelength, whereas NRs of high aspect ratio (~3) were fixed by the laser of 1064 nm. Most interestingly, in the case of 1064 nm wavelength, the majority of NRs were oriented to be parallel to the polarization direction of the azimuthal and radial (polarized) beams. Furthermore, many head-to-tail pairs of Ag NRs were observed (more than 60% of the fixed NRs), as indicated by the red arrows in Figs. 2c and 2e.

In order to understand the phenomena observed in Fig. 2, we theoretically evaluated the light-induced force on Ag NRs of different aspect ratios (sphere, Ag NRs of aspect ratio 2 and 3) in Fig. 3 (See **Methods** for more details). Two types of forces are shown here. One is the dissipative force arising from the photon momentum transfer

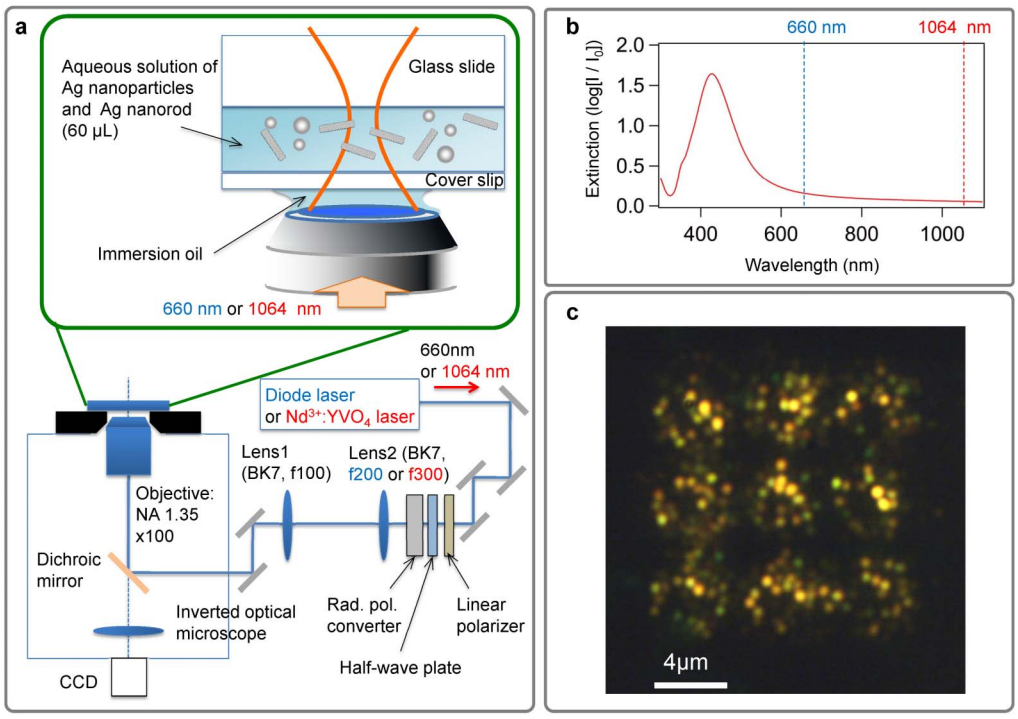

Figure 1 | Experimental setup and optical image of doughnut-like microstructures consisting of selectively assembled Ag nanoparticles. a, Aqueous solution of Ag nanoparticles (NPs) of various shapes and sizes, including Ag nanorods (NRs), are dropped between a substrate (glass slide) and a cover slip. A red diode laser (wavelength = 660 nm, power = 12.0 mW) or a Nd^{3+}:YVO_4 laser (wavelength = 1064 nm, power = 23.8 mW) is used as the light source for optical tweezing and is focused on the substrate surface for the fixation of Ag NRs. An oil immersion lens is used as the objective lens for laser focusing. b, Extinction spectrum of the suspension of Ag NPs. c, Dark-field optical image (scattering image) of ring-like arrangement of Ag NPs produced under the irradiation of radially polarized Nd^{3+}:YVO_4 laser with diameter ~2 μm.

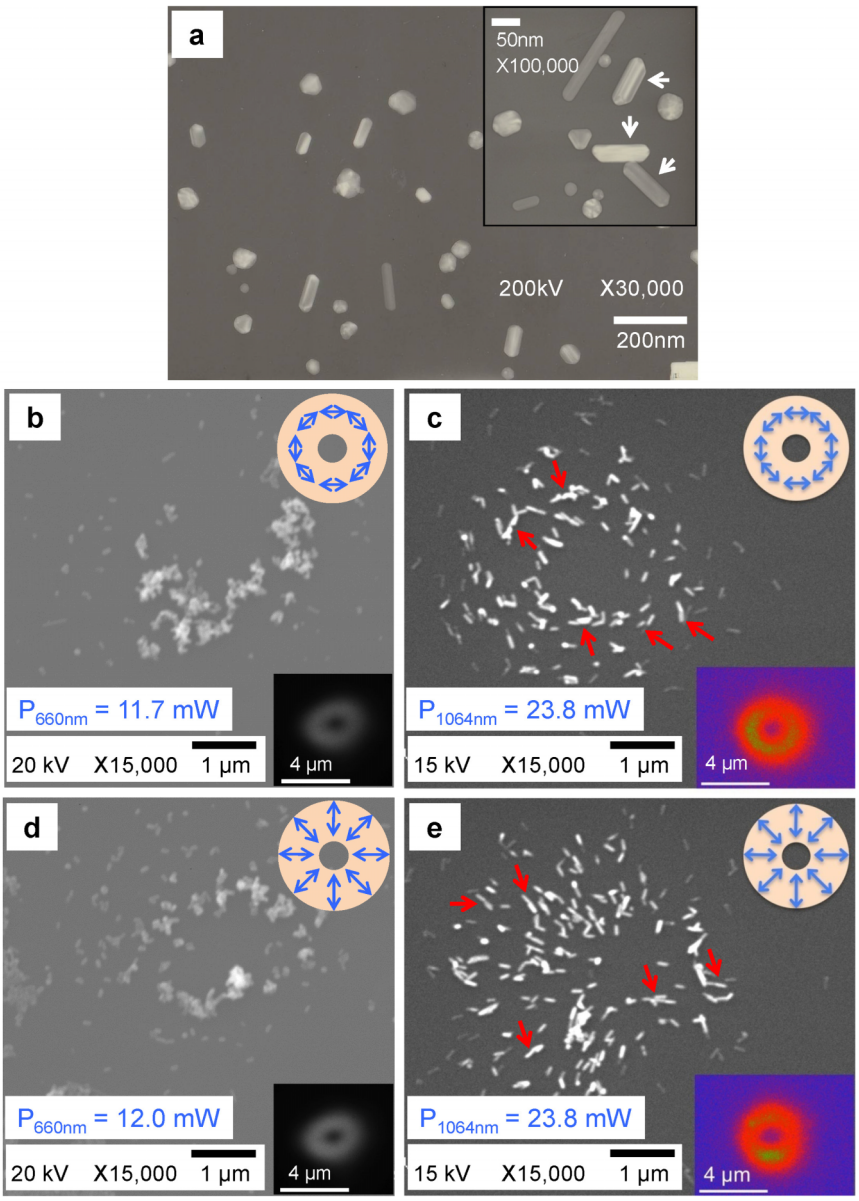

Figure 2 | Electron microscope images of the Ag nanorods before and after selection by doughnut laser beams with different wavelengths. a, Transmission electron microscope (TEM) image of Ag NPs used in this study without laser irradiation. Inset: enlarged view. b, c Scanning electron microscope (SEM) images of Ag NRs selected by the azimuthally polarized doughnut beam. d, e SEM images of Ag NRs selected by the radially polarized doughnut beam. Beams of 660 nm and 1064 nm wavelengths were used for b, d and c, e, respectively. The insets of b, c, d and e show the intensity distribution of the doughnut beam, as visualized by using fluorescence; and a schematic of the respective polarization.

in Figs. 3b and 3e, which pushes objects toward the laser propagation direction ($+z$-direction at {A} in Figs. 3a and 3d). The other is the gradient force (Figs. 3c and 3f) that is proportional to the light intensity gradient ($-x$-direction at {B} in Figs. 3a and 3d). The gradient force shown in Figs. 3c and 3f attracts NRs toward the high intensity region leading to the trapping condition when the laser wavelength is longer than the resonance of the LSP corresponding to the peak of dissipative force in Figs. 3b and 3e. In the calculation, the long axis (length) and the short axis (width) of Ag NRs with high aspect ratio were set as 120 nm and 40 nm (in reference to white arrows in the inset of Fig. 2a corresponding to NRs selected in Figs. 2c and 2e), whereas the length and width of Ag NRs with low aspect ratio were 80 nm and 40 nm (Figs. 2b and 2d). The refractive index of the surrounding medium was set to 1.33 (the value of water). With experimentally used laser power, the optical potential well for Ag NRs of high aspect ratio parallel to the light polarization is much deeper than the available thermal energy k_BT, (**See Supplementary Figures S1b and S1d**; an indication of the strength of fluctuations in the suspension: $k_BT = 26$ meV, where k_B is the Boltzmann constant, and the temperature $T = 298$ K). Whilst the potential wells for the spherical Ag NPs and the perpendicular Ag NRs are shallower, the large trapping potential of the parallel Ag NRs results in a more effective selection process under the thermal fluctuations of k_BT. As shown in Figs. 3b and 3e, at 1064 nm, the dissipative force on the parallel Ag NR of high aspect ratio (40 : 120 nm) is much greater than that on the spherical Ag NP, the perpendicular Ag NR, and the Ag NR of low aspect ratio (40 : 80 nm). Furthermore, when multiple Ag NRs are closely spaced and parallel to the polarization, the gradient force and the dissipative force for a pair of Ag NRs is greater than for the case of a single NR due to a redshift of the LSPs approaching the wavelength of the Nd^{3+}:YVO_4 laser. It is expected that the potential wells become deeper for more NRs aligned parallel to the polarization, and that the attractive and repulsive interparticle light-induced force[12,13] (**Supplementary Figures S2–S3**) have an

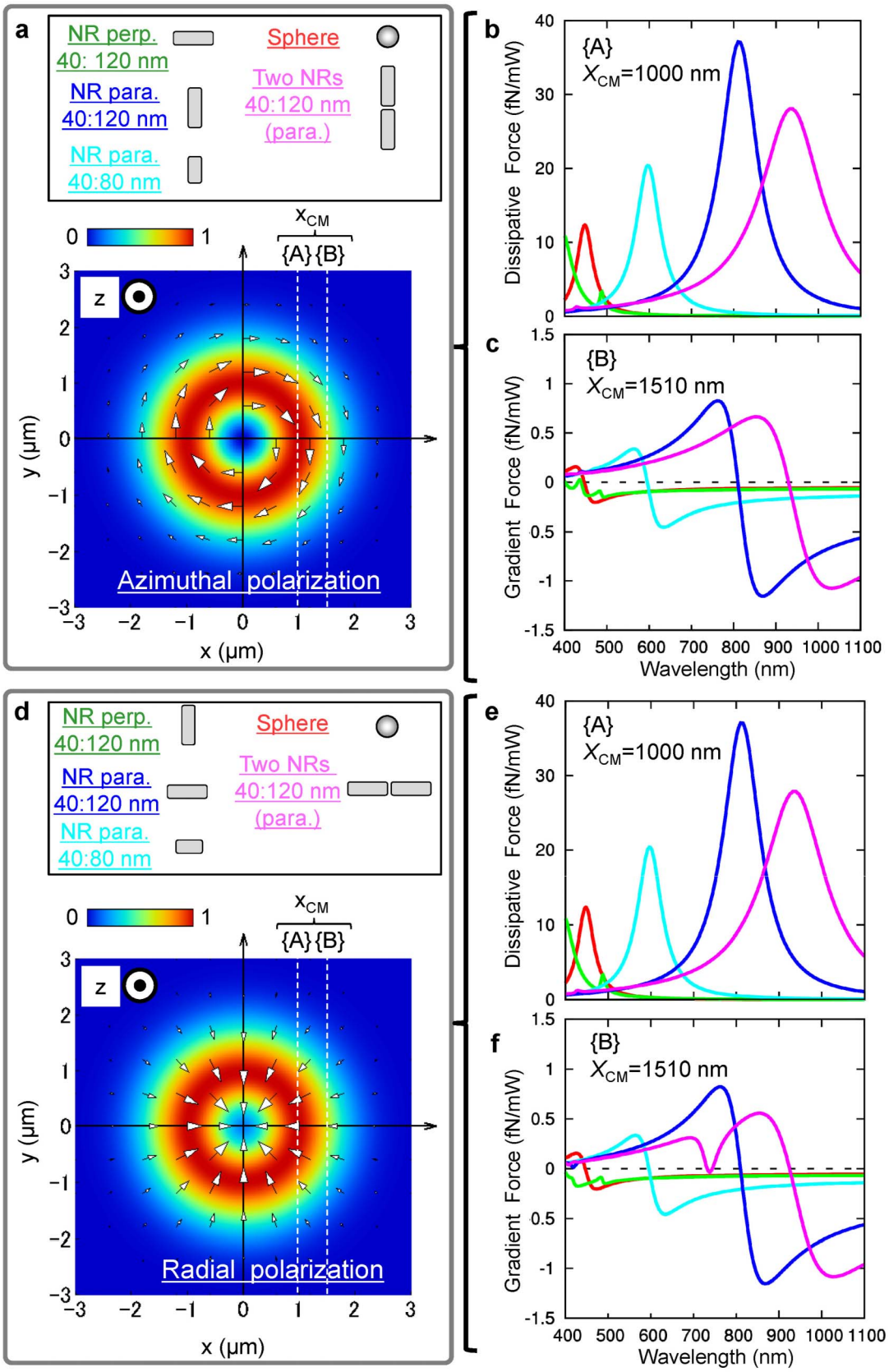

Figure 3 | Calculated spectra of the light-induced forces on Ag nanostructures. a, d, The schematic geometries of a spherical NP (60 nm in diameter), a single NR with low aspect ratio (40 nm width, 80 nm length) or with high aspect ratio (40 nm width, 120 nm length) in azimuthally and radially polarized beams, respectively. A pair of Ag NRs of high aspect ratio with 30 nm separation is also considered. The text colours correspond to lines in spectra. b, e, Dissipative force on Ag nanostructures whose centre of mass was located at {A}: (X_{CM} = 1000 nm, Y_{CM} = 0, Z_{CM} = 0), with the highest light intensity. c, f, Gradient force on a spherical NP, a single NR, and two NRs whose centre of mass was located at {B}: (X_{CM} = 1510 nm, Y_{CM} = 0, Z_{CM} = 0), with the steepest gradient of light intensity outside of the doughnut.

effect on the orientation. These results indicate that a group of Ag NRs with a particular aspect ratio and orientation can be efficiently extracted by resonant light-induced force aided by thermal fluctuations. Assembling processes under the irradiation of azimuthal and radial beams were also simulated by Monte Carlo method with self-consistently determined light-induced force (Figs. 4c and 4d, see also **Supplementary Movies S2 and S3**) that well explain the experimental results. Several Ag NRs are coupled with inter-object light-induced force and aligned parallel to the polarizations with a certain disorder arising from the thermal fluctuations. Furthermore, the area of assembled structure of Ag NRs can be scaled down if more tightly focused beam (**Supplementary Figure S5**) or the near-field APVBs[31]

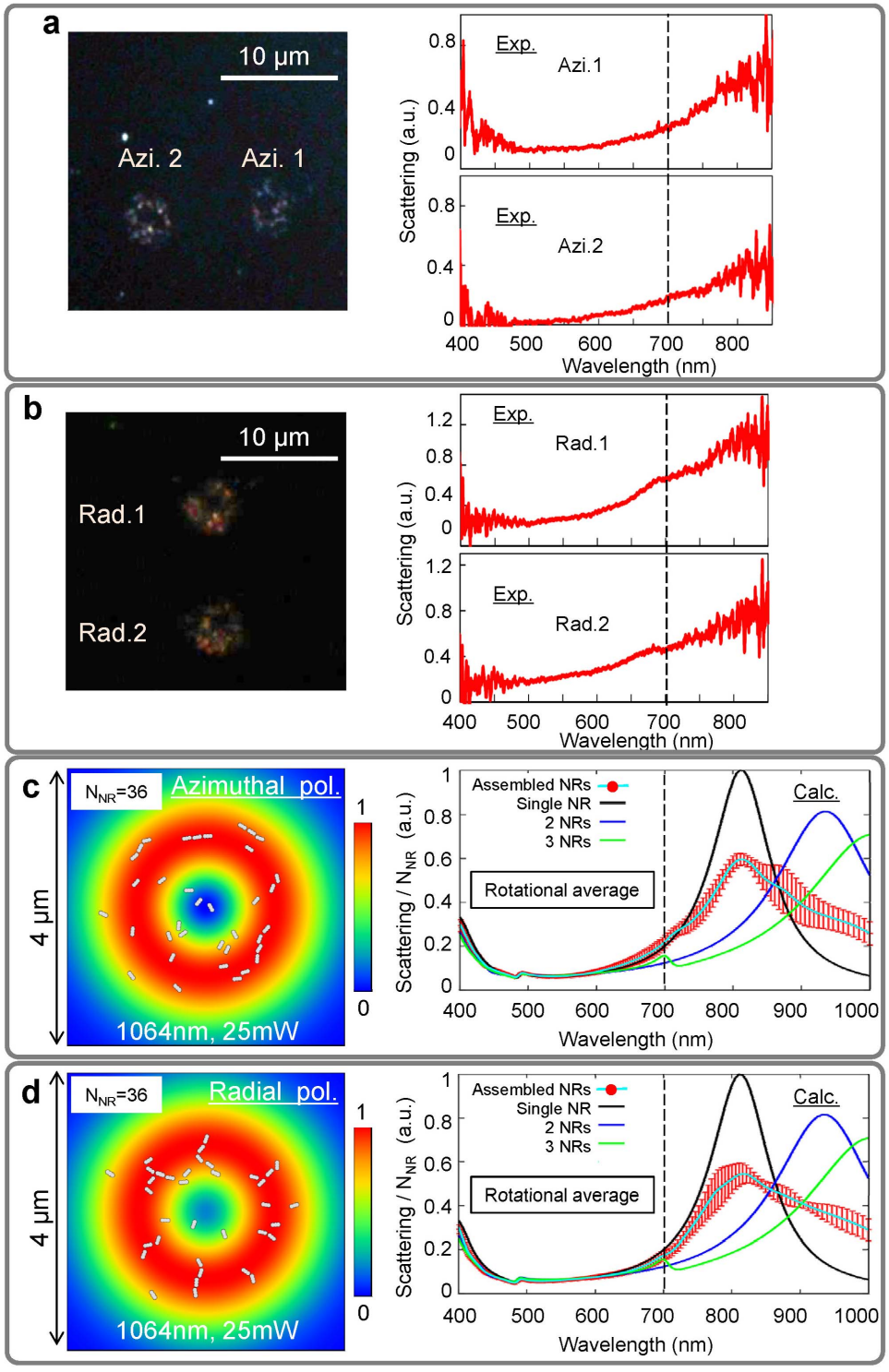

Figure 4 | Scattering from collective plasmonic modes of assembled Ag nanorods. a and b Scattering images, and the corresponding scattering spectra of Ag NRs densely assembled by 6 minutes irradiation of the azimuthally and radially polarized beams. c and d Calculated spectra of the total scattering from assembled Ag NRs by azimuthal and radial beams under the configuration obtained by Monte Carlo simulation on the left. The number of NRs is N_{NR} = 36. Also, spectra of a single Ag NR, and a head-to-tail array of two or three Ag NRs (with 30 nm separations) are shown together. In each line, the rotational average in *xy*-plane was taken under linear polarized light (red vertical bars in watery line indicate standard deviation in rotational average).

are utilized. Also, similar selective assembling of Ag NRs with particular aspect ratio was observed under the irradiation of a single Gaussian beam with wavelength of 660 nm or 1064 nm (See **Supplementary Figure S6–S7**). In the experiment using the 1064-nm beam, the orientations of selectively trapped AgNRs showed parallel orientation to the beam polarization direction similarly to the results for doughnut beams (**Supplementary Figure S6a**). These results indicate that we can control the orientations of selected Ag NRs by changing the spatial distributions of polarization and intensity of an irradiated beam. Time dependence of assembling of Ag NRs by 660 nm Gaussian beam was also investigated, where the number of Ag NRs increases for longer irradiation time. Within the given irradiation times, the thermal deformation can be almost neglected even near the LSP resonance condition of NRs of low aspect ratio. These results strongly support the selective arrangement of Ag NRs reflecting the designed properties of manipulation light sources and leading to optimum response to them.

Discussion

In order to understand the optical properties of the selectively assembled Ag NRs, their light scattering images and spectra were observed by dark-field optical microscopy (Fig. 4). The assembled Ag NRs with a ring-like shape appeared in optical images, as shown in Figs. 4a and 4b, with a corresponding scattering spectrum that had broad peak structures of LSP resonance from visible to infrared region. This behaviour is significantly different from the peak in the extinction of the original Ag NP suspension as shown in Fig. 1b owing to the selective deposition of NRs with high aspect ratios (see **Supplementary Figure S4**). In this case, the LSP of a single Ag NR should have a peak at 800 nm in water. As discussed in the previous paragraph, however, if multiple Ag NRs are closely spaced and fixed on the substrate it is expected that a large redshift of the LSP resonance will occur. For example, numerical simulations showed that when a pair of Ag NRs were aligned in the coaxial direction and spaced 30 nm apart, the LSP resonance moved to about 920 nm (Figs. 4c and 4d (right)). These numerically evaluated scattering spectra of assembled structure have similar shape as those in the experiment in Figs. 4a and 4b (right). In addition, a small peak appears at 700 nm in Fig. 4b (right) is considered as an optical forbidden mode of three NRs from the calculation (vertical broken line). These results imply that the multiple Ag NRs exhibit significantly strong electromagnetic coupling. Although the scattering spectra in Figs. 4a and 4b do not show remarkable difference in the measured wavelength range (400–900 nm) between two nanostructures of Ag NRs assembled by radial and azimuthal polarizations, numerical simulations under a condition of higher initial density of Ag NRs provided clearly different spectra for respective polarizations. It was confirmed that the Ag NRs assembled by the radially polarized beam showed prominent red-shifted collective modes of LSPs resonant with the irradiated light and a spectral broadening due to the strong confinement in the radial direction was more pronounced than the result of azimuthally polarized beam.

The results and discussion presented here will pioneer the innovative approach to selective assembling and separating analysis of various nanostructures with properties desired in the wide field of nanotechnology, for example, the nanoscale optical circuits[32], the high performance LHA for solar cells[33], the medical applications[34], the biosensors and the catalysts[35].

Methods

Optical setup. The experimental setup for the present study is illustrated in Fig. 1. A linearly polarized CW laser with a TEM_{00} transverse mode was used as the light source for optical manipulation (a diode laser with 660-nm output wavelength or an Nd^{3+}:YVO_4 laser with 1064-nm output wavelength). The beam profile and polarization were simultaneously modified by a liquid crystal (LQ) polarization converter (ARCoptix, Switzerland) to produce a doughnut-shaped beam with either azimuthal or radial polarization. By changing the applied voltage, the two polarizations were reciprocally converted without causing optical misalignment due to mechanical contact to the LQ device. The doughnut beam was focused onto the sample solution by an objective lens (NA 1.35, ×100, Olympus, Japan) attached to an inverted optical microscope (IX-70, Olympus, Japan). The spot size at the sample plane of the objective was controlled using a pair of lenses (lens 1 and 2). The intensity profile of the doughnut beam was estimated by detecting the fluorescence intensity distribution of an amorphous thin film of a fluorescent material excited either via two-photon absorption of 1064-nm laser beam or via one-photon absorption of the 660-nm beam.

Preparation of the colloid solution. The Ag NP colloidal solution was prepared by reduction of Ag ions in a $AgNO_3$ aqueous solution by sodium citrate at ~373 K, according to a previously reported procedure[30]. The shape and size of the synthesized Ag NPs were characterized by a scanning electron microscope (SEM, JSM-6060, JEOL, Japan) at acceleration voltages of 15–20 kV, and a transmission electron microscope (TEM, JEM-2000FXII, JEOL, Japan) operating at an acceleration voltage of 200 kV with a Cu microgrid (200 mesh, 6511, Nisshin EM, Japan). The samples for SEM imaging were coated by osmium to improve the conductivity.

Glass slide preparation. Glass slides (S-1111, Matsunami, Japan) were well washed with acetone before use. 60 μL of the Ag NP colloid was dropped onto a washed glass slide and covered with a cover slip. The doughnut beam was focused onto the Ag NP colloid solution sandwiched between the glass slide and cover slip so that the focal point of the doughnut beam was located on the surface of the glass slide. Ag NRs were assembled and deposited on the surface of the glass slides by radiation pressure of the Nd^{3+}:YVO_4 doughnut beam. After deposition, the glass slide was washed with ultrapure water and dried in an experimental room and the remaining Ag NPs were observed by SEM.

Scattering spectra. The scattering spectra of Ag NRs assembled on the glass substrate were obtained with a miniature fibre-optic spectrometer (USB4000, (Grating#3) SLIT-25, detector range: 200–1100 nm, Ocean Optics, USA,) and Halogen lamp as a white light source, which was connected to an optical microscope (ECLIPSE 80i, NIKON, Japan) via an optical fibre (core diameter: 50 μm).

Theoretical method. To evaluate the optical spectra, the spatial distribution of the response field around the Ag NRs and the force exerted on the Ag nanostructures, we evaluated the response field **E**, and induced polarization **P**, of Ag nanostructures from the solution of the relevant Maxwell equations. Using a discretized integral method[13] and modelling the spherical Ag NP as a spherical cell and the Ag NR as an assembly of cubic cells:

$$\mathbf{E}_i = \mathbf{E}_i^{(0)} + \sum_{j\neq i}^{N} \mathbf{G}^{\mathrm{hm}}(\mathbf{r}_{ij})\mathbf{P}_j V_j + S_i \mathbf{P}_i, \tag{1}$$

$$\mathbf{P}_j = \chi_j \mathbf{E}_j, \tag{2}$$

where N is the number of cells, V_j is the volume of each cell, $\mathbf{E}_i^{(0)}$ is the electric field component of an incident optical field, $\mathbf{G}^{\mathrm{hm}}$ is the Green's function in a homogeneous medium, and χ_j is the electric susceptibility. The integral $S_i = \int_{V_i} d\mathbf{r}' \mathbf{G}^{\mathrm{hm}}(\mathbf{r}_i - \mathbf{r}')$ for $i = j$ as the self-term in Equation (1) was analytically calculated. By substituting the obtained **E** and **P** as solutions of the simultaneous Equations (1) and (2) into the general expression of light-induced-force[12]:

$$<\mathbf{F}_i> = (1/2)\mathrm{Re}[\sum_{\omega} \int_{V_i} d\mathbf{r}(\nabla \mathbf{E}(\mathbf{r},\omega)^*)\cdot \mathbf{P}(\mathbf{r},\omega)], \tag{3}$$

we can evaluate the gradient force, dissipative force, and interparticle light-induced force (the spectral properties of these components are shown in **Supplementary Figures S1–S3**). The total light momentum transfer rate is proportional to the extinction. The extinction spectrum of the total system can be calculated by evaluating the sum of the radiation pressure $<\mathbf{F}_j^{\mathrm{pw}}>$ on all of the nanostructures under irradiation of a propagating plane wave as $<\mathbf{F}_{\mathrm{total}}^{\mathrm{ext}}> = \sum_j <\mathbf{F}_j^{\mathrm{pw}}>$, which is the sum of scattering and absorption forces. Finally, the total scattering spectra of the assembled Ag NRs can be obtained by evaluating $<\mathbf{F}_{\mathrm{total}}^{\mathrm{scat}}> = <\mathbf{F}_{\mathrm{total}}^{\mathrm{ext}}> - <\mathbf{F}_{\mathrm{total}}^{\mathrm{abs}}>$, where $<\mathbf{F}_{\mathrm{total}}^{\mathrm{abs}}> = \sum_j (V_j/2)\mathrm{Im}[\mathbf{k}(\mathbf{P}_j^* \cdot \mathbf{E}_j)]$ is the absorption component (**k** is the wave vector of the plane wave). In addition, the Drude type electric susceptibility is used to determine the χ_j of Ag nanostructures whose parameters were determined from the experimental results and the published optical constants of Johnson and Christy[29]. The incident electromagnetic field of the axially-symmetric vector beam (Figs. 3a and 3d) was determined from the general expressions without paraxial approximation[20].

Furthermore, in order to find the final configuration of Ag NRs under the irradiation of doughnut beams as shown in Fig. 4c (left) and 4d (left) (also in **Supplementary Movies S2 and S3**), we use the Monte Carlo simulation taking into account self-consistently determined light-induced force with Equations (1)–(3). The variation of optical potential is given as $dE_{\sigma+1} = -\sum_i <\mathbf{F}_i> \cdot d\mathbf{r}_i$ after the random positional changes of Ag NR during the σth and $(\sigma + 1)$th steps. If $dE_{\sigma+1} \leq 0$ is satisfied, the $(\sigma + 1)$th state is always adopted since the energy of this state is lower

than that of the σth step. On the other hand, if $dE_{\sigma+1} > 0$ is satisfied, the $(\sigma + 1)$th state is adopted with the probability of $p = \exp(-dE_{\sigma+1}/k_BT)$ or the configuration does not change since the energy of this state is higher than the σth step. The variations of potential due to random rotational motions of Ag NRs are also considered. Repeating these procedures, we can find the more stable spatial configuration of assembled Ag NRs. Each Ag NR is described with three combined cubic cells.

1. Nicolis, G. & Prigogine, I. *Self-Organization in Non-Equilibrium Systems* (Wiley, New York, 1977).
2. Rabani, E., Reichman, D. R., Geissler, P. L. & Brus, L. E. Drying-mediated self-assembly of nanoparticles. *Nature* **426**, 271–274 (2003).
3. Shevchenko, E. V., Talapin, D. V., Kotov, N. A., O'Brien, S. & Murray, C. B. Structural diversity in binary nanoparticle superlattices. *Nature* **439**, 55–59 (2006).
4. Rothemund, P. W. K. Folding DNA to create nanoscale shapes and patterns. *Nature* **440**, 297–302 (2006).
5. Bahatyrova, S. *et al*. The native architecture of a photosynthetic membrane. *Nature* **430**, 1058–1062 (2004).
6. Scheuring, S. & Sturgis, J. N. Chromatic adaptation of photosynthetic membranes. *Science* **309**, 484–487 (2005).
7. Kiang, N. Y., Siefert, J. & Govindjee Blankenship, R. E. Spectral signatures of photosynthesis. I. Review of earth organisms. *Astrobiology* **7**, 222–251 (2007).
8. Ashkin, A. Acceleration and trapping of particles by radiation pressure. *Phys. Rev. Lett.* **24**, 156–159 (1970).
9. Ito, S., Yoshikawa, H. & Masuhara, H. Laser manipulation and fixation of single gold nanoparticles in solution at room temperature. *Appl. Phys. Lett.* **80**, 482–484 (2002).
10. Iida, T. & Ishihara, H. Theoretical Study of the Optical manipulation of semiconductor nanoparticles under an excitonic resonance condition. *Phys. Rev. Lett.* **90**, 057403 (1–4) (2003).
11. Inaba, K. *et al*. Optical manipulation of CuCl nanoparticles under an excitonic resonance condition in superfluid helium. *Phys. Stat. Sol. (b)* **243**, 3829–3833 (2006).
12. Iida, T. & Ishihara, H. Theory of resonant radiation force exerted on nanostructures by optical excitation of their quantum states: From microscopic to macroscopic descriptions. *Phys. Rev. B* **77**, 245319 (1–16) (2008).
13. Iida, T. Control of plasmonic superradiance in metallic nanoparticle assembly by light-induced force and fluctuations. *J. Phys. Chem. Lett.* **3**, 332–336 (2012).
14. Ito, S. *et al*. Confinement of photopolymerization and solidification with radiation pressure. *J. Am. Chem. Soc.* **133**, 14472–14475 (2011).
15. Tamura, M. & Iida, T. Fluctuation-mediated optical screening of nanoparticles. *Nano Lett.* **12**, 5337–5341 (2012).
16. Grier, D. G. A revolution in optical manipulation. *Nature* **424**, p. 810–816 (2003).
17. Jiang, Y., Narushima, T. & Okamoto, H. Nonlinear optical effects in trapping nanoparticles with femtosecond pulses. *Nature Phys.* **6**, 1005–1009 (2010).
18. Tsuboi, Y. *et al*. Optical trapping of quantum dots based on gap-mode-excitation of localized surface plasmon. *J. Phys. Chem. Lett.* **1**, 2327–2333 (2010).
19. Oron, R. *et al*. The formation of laser beams with pure azimuthal or radial polarization. *Appl. Phys. Lett.* **77**, 3322–3324 (2000).
20. Gu, B. & Cui, Y. Nonparaxial and paraxial focusing of azimuthal-variant vector beams. *Opt. Exp.* **20**, 17684–17694 (2012).
21. Selhuber-Unkel, C., Zins, I., Schubert, O., Sönnichsen, C. & Oddershede, L. B. Quantitative Optical Trapping of Single Gold Nanorods. *Nano Lett.* **8**, 2998–3003 (2008).
22. Pelton, M. *et al*. Optical trapping and alignment of single gold nanorods by using plasmon resonances. *Opt. Lett.* **31**, 2075–2077 (2006).
23. Tong, L., Miljković, V. D. & Käll, M. Alignment, Rotation, and Spinning of Single Plasmonic Nanoparticles and Nanowires Using Polarization Dependent Optical Forces. *Nano Lett.* **10**, 268–273 (2010).
24. Head, C. R., Kammann, E., Zanella, M., Manna, L. & Lagoudakis, P. G. Spinning nanorods - active optical manipulation of semiconductor nanorods using polarised light. *Nanoscale* **4**, 3693–3697 (2012).
25. Whiley, B. J. *et al*. Synthesis and Optical Properties of Silver Nanobars and Nanorice. *Nano Lett.* **7**, 1032 (2007).
26. Dicke, R. H. Coherence in Spontaneous Radiation Processes. *Phys. Rev.* **93**, 99–110 (1954).
27. Scheibner, M. *et al*. Superradiance of quantum dots. *Nature Phys.* **3**, 106–110 (2007).
28. Miyajima, K., Kagotani, Y., Saito, S., Ashida, M. & Itoh, T. Superfluorescent pulsed emission from biexcitons in an ensemble of semiconductor quantum dots. *J. Phys. Condens. Matter* **21**, 195802 (1–6) (2009).
29. Johnson, P. B. & Christy, R. W. Optical constants of the noble metals. *Phys. Rev. B* **6**, 4370–4379 (1972).
30. Lee, P. C. & Meisel, D. Adsorption and surface-enhanced raman of dyes on silver and gold sols. *J. Phys. Chem.* **86**, 3391–3395 (1982).
31. Kato, K., Ono, A., Inami, W. & Kawata, Y. Plasmonic nanofocusing using a metal-coated axicon prism. *Opt. Exp.* **18**, 13580–13585 (2010).
32. Engheta, N. Circuits with Light at Nanoscales: Optical Nanocircuits Inspired by Metamaterials. *Science* **317**, 1698 (2007).
33. Atwater, H. A. & Polman, A. Plasmonics for improved photovoltaic devices. *Nature Mat.* **9**, 205–213 (2010).
34. Weintraub, K. Biomedicine: The new gold standard. *Nature* **495**, S14–S16 (2013).
35. Tokonami, S., Yamamoto, Y., Shiigi, H. & Nagaoka, T. Synthesis and bioanalytical applications of specific-shaped metallic nanostructures: A review. *Anal. Chim. Acta* **716**, 76–91 (2012).

Acknowledgements

The authors (S.I. and T.Ii) would like to thank Prof. T. Tsutsui and Prof. H. Ishihara for kind encouragement and support. This work was supported by PRESTO from the JST; a Grant-in-Aid for Scientific Research (B) No. 23310079; a Grant-in-Aid for Young Scientists (A) No. 23681023; the Grants-in-Aid for Exploratory Research No. 23655072 and No. 24654091 from the JSPS; and Special Coordination Funds for Promoting Science and Technology from the MEXT (Improvement of Research Environment for Young Researchers (FY 2008-2012).

Author contributions

T.Ii. and S.I. initiated the research presented here, and equally contributed to designing the research. S.I., H.Y. and H.M. performed the optical assembling of Ag nanorods experiments. S.I., H.Y., T.H., K.N. and S.T. obtained the scanning electron microscope (SEM) images, transmission electron microscope (TEM) images, scattering images, and the measurements of spectra from Ag nanorods fixed on the substrate. T.It. produced original Ag nanoparticles. M.T., S.H., H.H. and T.Ii carried out the theoretical calculations. S.I. and T.Ii prepared the figures and the manuscript. All authors discussed the results and commented on the manuscript.

Additional information

Supplementary information accompanies this paper at http://www.nature.com/scientificreports

Competing financial interests: The authors declare no competing financial interests.

How to cite this article: Ito, S. *et al*. Selective Optical Assembly of Highly Uniform Nanoparticles by Doughnut-Shaped Beams. *Sci. Rep.* **3**, 3047; DOI:10.1038/srep03047 (2013).

SCIENTIFIC REPORTS

DOI: 10.1038/srep03802

SUBJECT AREAS:
SUB-WAVELENGTH OPTICS
NANOPHOTONICS AND PLASMONICS
NANOPARTICLES

SCIENTIFIC REPORTS:
3 : 3047
DOI: 10.1038/srep03047

Published:
25 October 2013

Updated:
27 February 2014

ERRATUM: Selective Optical Assembly of Highly Uniform Nanoparticles by Doughnut-Shaped Beams

Syoji Ito, Hiroaki Yamauchi, Mamoru Tamura, Shimpei Hidaka, Hironori Hattori, Taichi Hamada, Keisuke Nishida, Shiho Tokonami, Tamitake Itoh, Hiroshi Miyasaka & Takuya Iida

The incorrect versions of Supplementary Movies 2 and 3 were published with the original Article. In the original versions of Supplementary Movies 2 and 3 the size of the background colour maps were modified during the file conversion process. The numerical results contained in the videos were correct.